J. Automation & Systems Engineering

Regular paper

Direct Torque Control of an Electronic Differential for Electric Vehicle with Separate Wheel Drives

K. Hartani, M. Bourahla, Y. Miloud and M. Sekkour

This paper presents the system analysis, modeling and simulation of electronic differential for electric vehicle with two separate wheel drives based on direct torque control (DTC). The proposed traction system consists of two permanent magnet synchronous (PMS) machines that ensure the drive of the two back driving wheels. The control structure called independent machines for speed control permits however the achievement of an electronic differential. Direct torque control scheme is used to control the electronic differential to achieve high accuracy in curved roads.

Keywords: Electric vehicle, electronic differential, direct torque control, permanent magnet synchronous motor.

1. INTRODUCTION

Traction drive used in electric vehicles can be divided into two categories, (i) single drive system, and (ii) multi-drive systems. With multi-drive systems the motor controllers must additionally be configured to provide an electronic differential effect i.e. they must also perform a similar function as their mechanical differential counterpart. Thus the electronic differential must take account of the speed difference between the two wheels when cornering.

The traction system proposed consists of two permanent magnet synchronous machines (PMSM) that ensure the drive of the two back driving wheels. This system is called multi-machine multi-converter systems [1]. They are recognized through the existence of the coupling system type either of an electric nature, a magnetic and/or mechanical one used in several electric machines propulsing the vehicle. The proposed control structure [2] called “independent machines” for speed control permits the achievement of an electronic differential based on direct torque control (DTC).

2. PROPOSED TRACTION SYSTEM

The usual configuration of electrical or non-electrical vehicles present only one traction motor driving two wheels, using a differential gear. In this work, a structure of vehicle was adapted to obtain a vehicle with two independent wheel drives, Figure 1. This configuration with two traction wheels in the vehicle may presents some advantages such as increasing the vehicle power with a better weight distribution and no power loss in the differential gear [3].

The multi-machine systems are characterized by the coupling of different electromechanical conversion systems. The system represented by the Figure 1.b is characterized by only one coupling. It is illustrated by Figure 2. In order to realize the electronic differential, the control structure “independent machines” is applied to the

University Center Dr. Moulay Tahar of Saida, Algeria.
University of Science and Technology Mohamed Boudiaf of Oran, Algeria.

traction system of two driving wheels by a speed control, Figure 3.

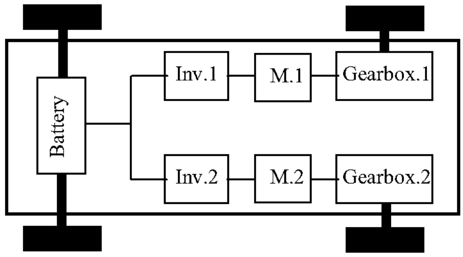

Figure 1: Vehicle structure with two independent rear wheel drives.

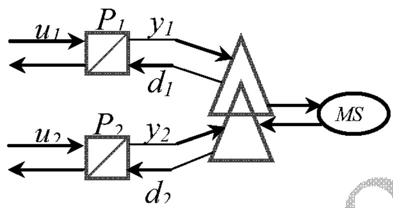

Figure 2. Studied topology.

2. A. Independent machine control structure

This structure is composed of two machines controlled independently as two single machine structures. For each machine we can impose different speed reference ($\Omega_{rRref} \neq \Omega_{rLref}$) by using two static converters. These machines are uncoupled through the control structure and reject all disturbances like single machine control [4]. The principle of this control is illustrated by Figure 3.

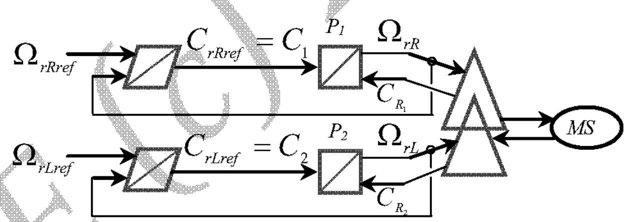

Figure 3. Independent machine structure.

3. GLOBAL SYSTEM MODELING

The proposed electric vehicle drive system has two PMS motors for the rear wheel drives, Figure 4. With multi-drive systems, the motor controllers must additionally be configured to provide an electronic differential effect i.e. they must also perform a similar function as their mechanical differential counterpart. Thus, the electronic differential must take account of the speed difference between the two wheels when cornering. The system uses the vehicle speed and steering angle as input parameters and calculates the required inner and outer wheel speeds where the two rear wheels are controlled independently by two PMS motors. Figure 5 shows the proposed system control for the electronic differential based on DTC control.

3.A. Modeling of Electronic differential

The considered propulsion system architecture permits to develop an electronic differential (Figure 6.a) assuring that, in straight right trajectory, the two wheel drives roll exactly at the same velocity and, in curve, the difference between the two velocities assures a vehicle trajectory. Since the two rear wheels are directly driven by two separate motors, the speed of the outer wheel will require to be higher than the speed of the inner wheel during steering application (and vice versa), if tyre "rubbing" is to be avoided. Figure 6.b. shows the vehicle structure describing a curve, where L_w represents the wheelbase, δ the steering angle, d_w the distance between the wheels of the same axle and ω_R and ω_L the angular speeds of the right and the left wheel drives respectively.

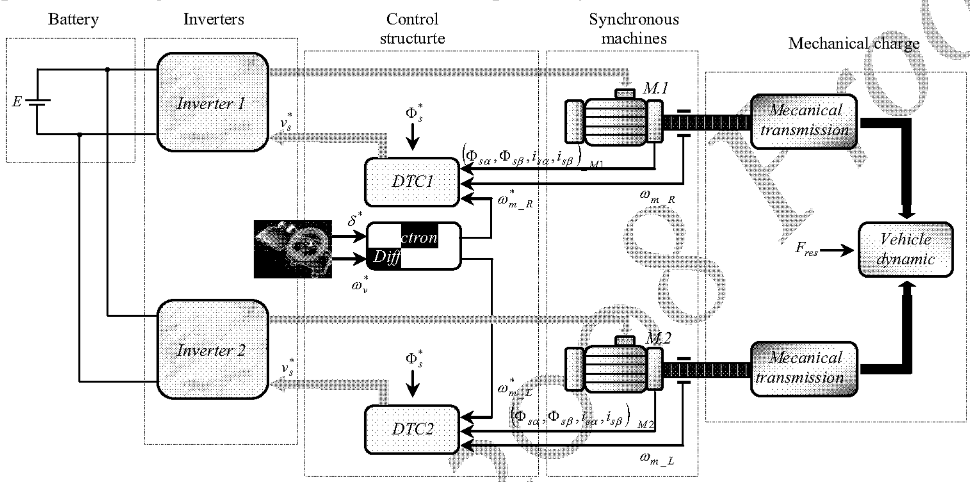

Figure 4. The driving wheels control system.

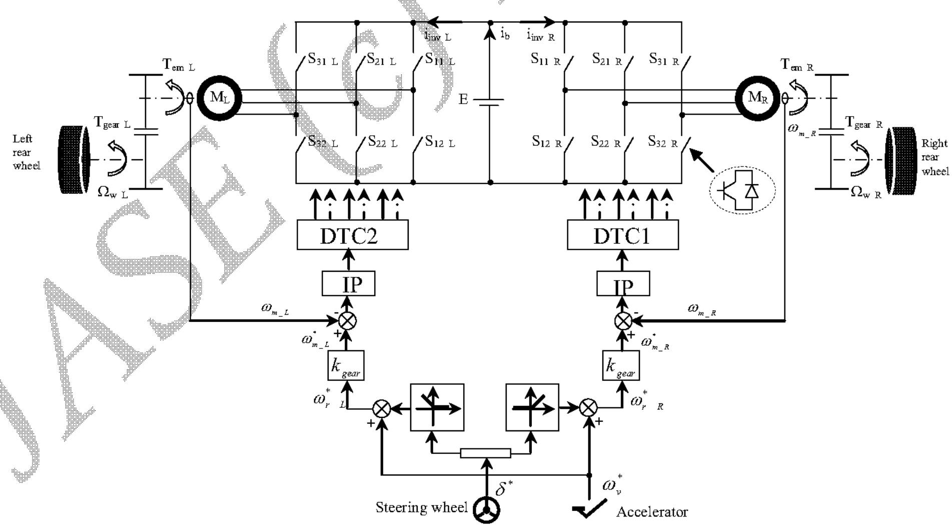

Figure 5. Components of proposed system control.

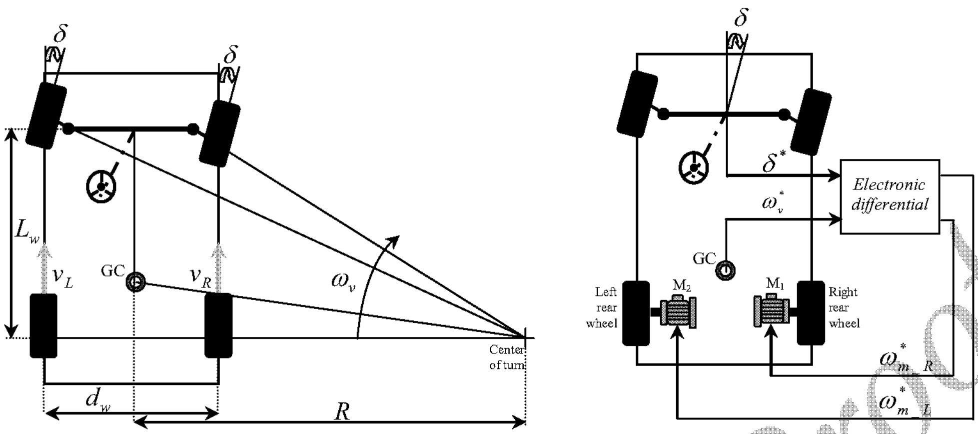

Figure 6. Vehicle structure in curve.

Accordance to Figure 6, the linear speed of each wheel drive is expressed as a function of the vehicle speed and the radius of curve, by equations (1) and (2)

$$v_L = \omega_v \left(R + \frac{d_w}{2} \right) \qquad (1)$$

$$v_R = \omega_v \left(R - \frac{d_w}{2} \right) \qquad (2)$$

The radius of curve depends on the wheelbase and steering angle (equation (3)):

$$R = \frac{L_w}{\tan \delta} \qquad (3)$$

Substituting (3) in equations (1) and (2), we obtain the angular speed in each wheel drive (equation (4) and (5)):

$$\omega_{r\_L} = \frac{L_w + d_w/2 . \tan \delta}{L_w} \omega_v \qquad (4)$$

$$\omega_{r\_R} = \frac{L_w - d_w/2 . \tan \delta}{L_w} \omega_v \qquad (5)$$

The difference between the angular speeds of the wheel drives is express by equation (6). The signal of the steering angle indicates the curve direction (7).

$$\Delta\omega = \omega_{r\_L} - \omega_{r\_R} = \frac{d_w . \tan \delta}{L_w} \omega_v \qquad (6)$$

$$\begin{cases} \delta \rangle 0 & \Rightarrow \quad Turn \;\; right \\ \delta = 0 & \Rightarrow \quad Straight \;\; ahead \\ \delta \langle 0 & \Rightarrow \quad Turn \;\; left \end{cases} \qquad (7)$$

When the vehicle arrives at the beginning of a curve, the driver applies a steering angle on the wheels. The electronic differential however acts immediately on the two motors reducing the speed of the inner wheel, and increases the speed of the outer wheel, Figure 6. The driving wheel angular speeds are:

$$\omega^*_{r\_L} = \omega_v + \frac{\Delta\omega}{2} \tag{8}$$

$$\omega^*_{r\_R} = \omega_v - \frac{\Delta\omega}{2} \tag{9}$$

The speed references of the two motors are:

$$\omega^*_{m\_L} = k_{gear}\omega^*_{r\_L} \tag{10}$$

$$\omega^*_{m\_R} = k_{gear}\omega^*_{r\_R} \tag{11}$$

where k_{gear} is the gearbox ratio.

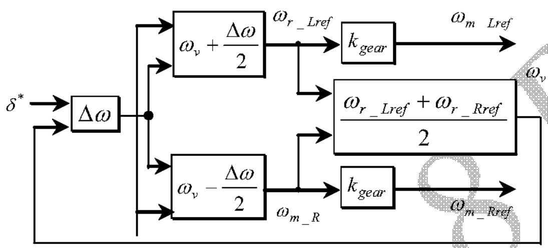

Figure 7. Block diagram of the electronic differential

3.B. Traction motor model

The PMSM model can be described in the stator reference frame as follows [5]:

$$\begin{cases} \frac{di_{s\alpha}}{dt} = -\frac{R_s}{L_s} i_{s\alpha} + \frac{\Phi_f}{L_s}\omega_m \sin\theta + \frac{1}{L_s} v_{s\alpha} \\ \frac{di_{s\beta}}{dt} = -\frac{R_s}{L_s} i_{s\beta} - \frac{\Phi_f}{L_s}\omega_m \cos\theta + \frac{1}{L_s} v_{s\beta} \\ \frac{d\omega_m}{dt} = -\frac{f}{J}\omega_m + \frac{p}{J}(T_{em} - T_r) \end{cases} \tag{12}$$

and the electromagnetic torque equation

$$T_{em} = \frac{3}{2} p\Phi_f \left(-i_{s\alpha} \sin\theta + i_{s\beta}\cos\theta\right) \tag{13}$$

3.C. Inverter model

In this electric traction system, we use a voltage inverter to obtain three balanced phases of alternating current with variable frequency. The voltages generated by the inverter are given as follows:

$$\begin{bmatrix} v_a \\ v_b \\ v_c \end{bmatrix} = \frac{E}{3} \begin{bmatrix} 2 & -1 & -1 \\ -1 & 2 & -1 \\ -1 & -1 & 2 \end{bmatrix} \begin{bmatrix} S_a \\ S_b \\ S_c \end{bmatrix} \tag{14}$$

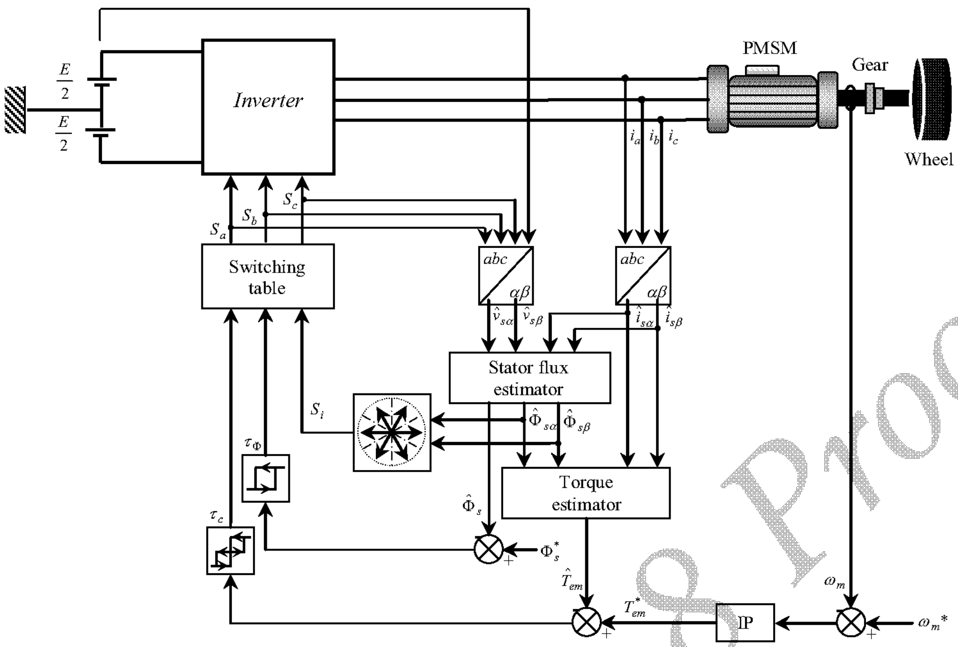

Figure 8. System block diagram of PMSM based DTC control.

3.D. Energy source

The source of energy is generally a Lithium-Ion accumulator's battery. Lithium-Ion battery technology offers advantages of specific energy, specific power, and life over other types of rechargeable batteries. [6, 7, 8, 9]

3.E. Vehicle dynamic

The total resistive force is defined as [10]

$$F_{res} = F_{roll} + F_{aero} + F_{slope} \tag{15}$$

and

$$F_{roll} = \mu m g \tag{16}$$

$$F_{aero} = \frac{1}{2}\rho C_D A_f V_h^2 \tag{17}$$

$$F_{slope} = m g p_{\%} \tag{18}$$

where F_{roll} is the rolling resistance, F_{aero} is the aerodynamic drag force and F_{slope} is the slope resistance.

4. PMSM DTC SYSTEM

Figure 8 illustrates the structure of a PMSM DTC system [11] control with an inner torque loop and an outer speed loop. In this system, two stator phase currents i_a and i_b and the DC-link voltage E are measured. The stator flux linkage components $\Phi_{s\alpha}$ and $\Phi_{s\beta}$, the flux linkage amplitude $|\Phi_s|$, the torque T_{em} and the flux angle θ_s can be determined as follow: [12]

$$\begin{cases} \Phi_{s\alpha} = \int_0^t \left(V_s - R_s i_{s\alpha}\right) dt \\ \Phi_{s\beta} = \int_0^t \left(V_s - R_s i_{s\beta}\right) dt \end{cases} \tag{19}$$

$$\Phi_s = \sqrt{\Phi_{s\alpha}^2 + \Phi_{s\beta}^2} \tag{20}$$

$$\theta_s = artg\left(\frac{\Phi_{s\beta}}{\Phi_{s\alpha}}\right) \tag{21}$$

$$T_{em} = \frac{3}{2} p\left(\Phi_{s\alpha} i_{s\beta} - \Phi_{s\beta} i_{s\alpha}\right) \tag{22}$$

The system basically comprises two controllers for flux linkage and torque control. The use of the flux controller is to maintain the flux amplitude within a narrow hysteresis and around the reference value Φ_s^*. The torque controller receives the information obtained from the torque calculated and compares this value with the output of a speed IP controller.

5. SIMULATION RESULTS

The PMSM DTC system illustrated in Figure 5 is simulated by using MATLAB/SIMULINK. The parameters used in this system are listed in the Appendix. Figure 9 shows the dynamic performance of the torque control loop of DTC system (without the speed loop), which is obtained by applying a variable torque command of 50 N.m magnitude. It can be seen that the DTC control is a more effective method for accurate control of the electromagnetic torque and the flux linkage. Figure 10 shows the starting performance of DTC system corresponding to a step speed command of 0-600 rd.s^{-1}.

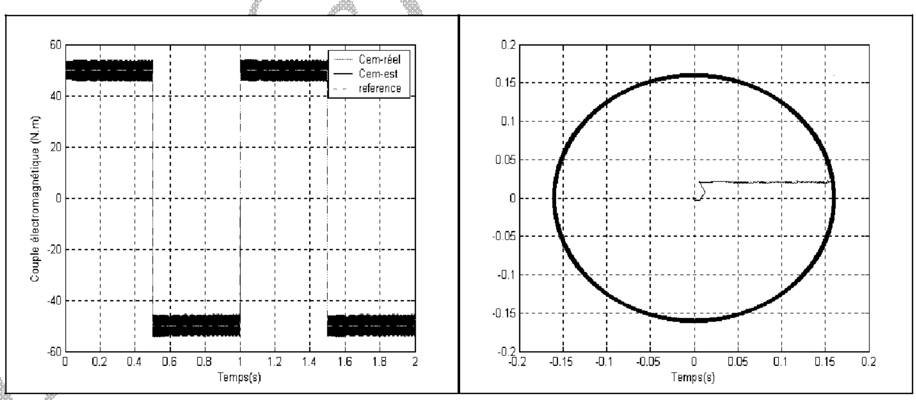

(a) Electromagnetic torque (b) Stator flux linkage trajectory

Figure 9. Simulated responses of PMSM DTC system under variable torque command

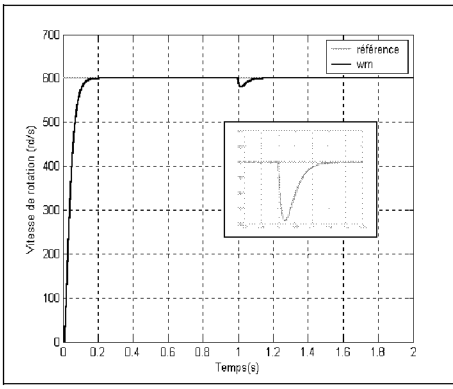

(a) Speed motor

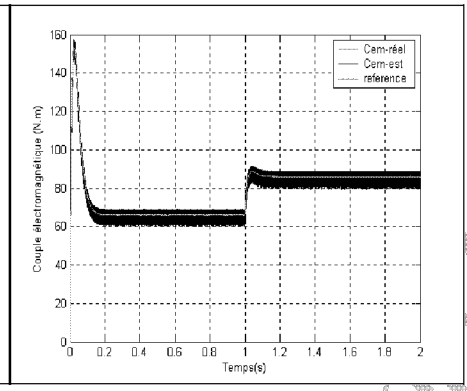

(b) Electromagnetic torque

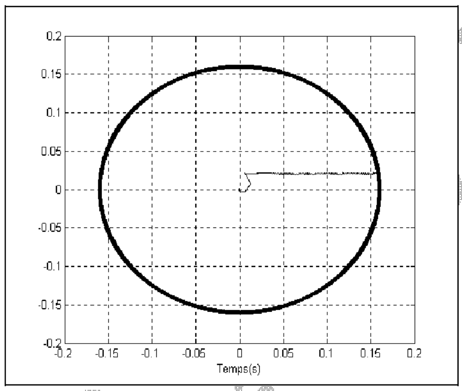

(c) Stator flux linkage

Figure 10. Simulated starting performances of PMSM DTC system

Now we simulate the whole system Figure 4 by taking in account the electronic differential for electric vehicle in both curved roads right and left.

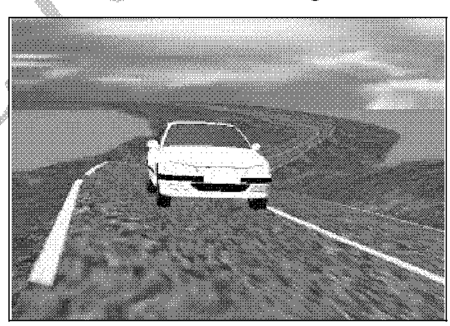

Figure 11. Vehicle on curved way

5.A. Curved road at right side with speed of $80km/h$

The vehicle is drived on a curved road on the right side with $80km/h$ speed. The assumption is that the two motors are not disturbed. In this case, the driving wheels follow different paths, and they turn in the same direction but with different speeds. The electronic differential acts on the two motor speeds by decreasing the speed of the driving wheel on the right side situated inside the curve, and on the other hand by increasing the wheel motor speed in the external side of the curve. The behaviour of these speeds is given by Figure 12(a) and 12(b).

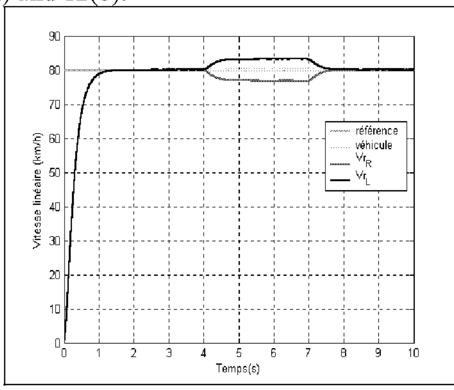

(a) Linear speeds

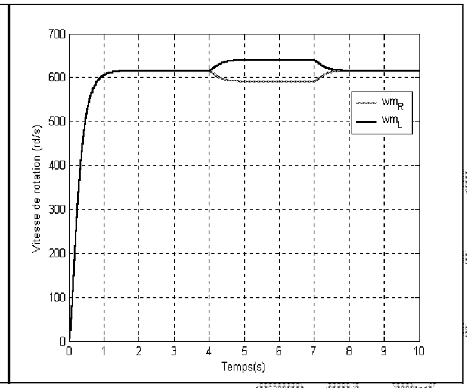

(b) Right and left wheel rotational speed

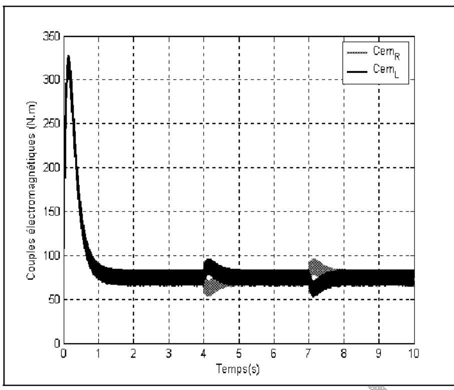

(c) Electromagnetic torques

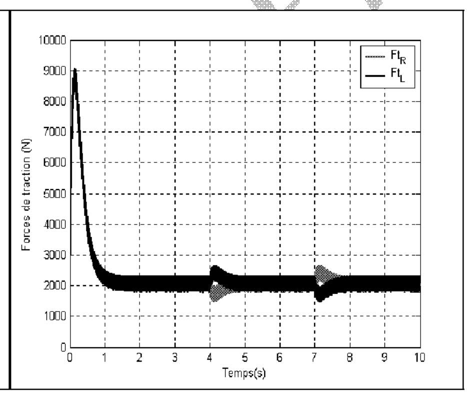

(d) Driving forces

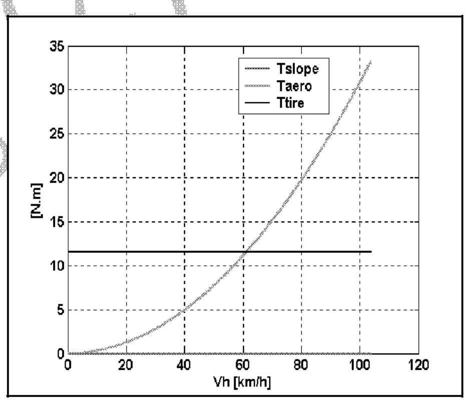

(e) Total resistive torque

Figure 12. Simulation results of curved road with right turn.

5.B. Curved road with left turn at a speed of $80km/h$

The vehicle is moving on a curved road with left turn at a speed of $80km/h$, Figure 13. It is assumed again that the two motors are not disturbed. In this case, the driving wheels follow different paths. They turn in the same direction but with different speeds. The left driving wheel turns at a speed less than that of the right.

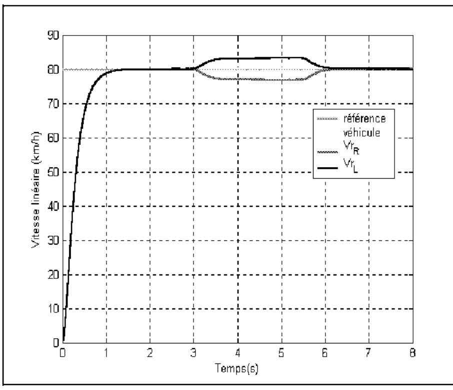

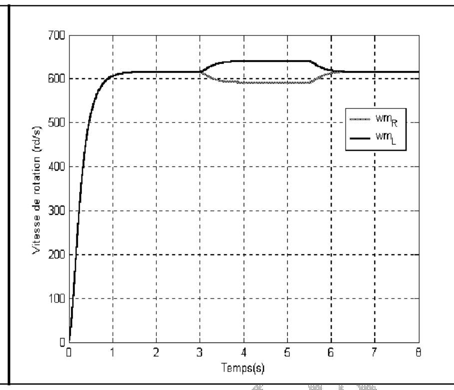

(a) Linear speeds (b) Right and left wheel rotational speed

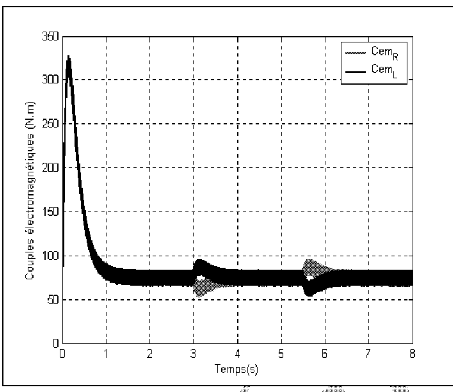

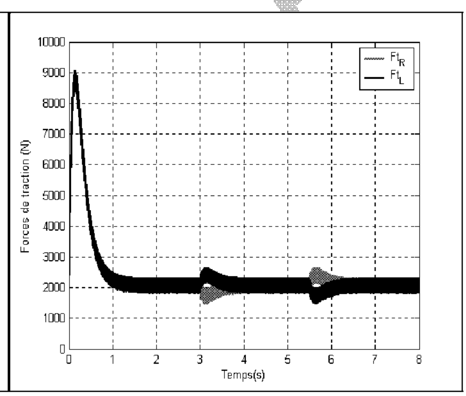

(c) Electromagnetic torques (d) Driving forces

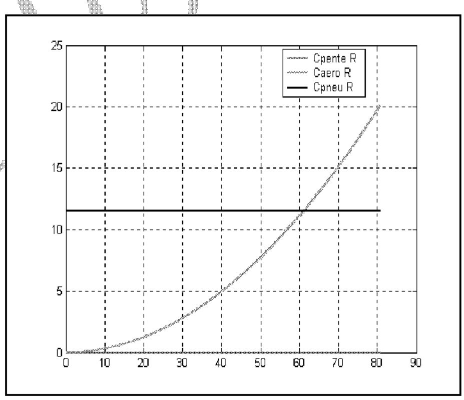

(e) Total resistive torque

Figure 13. Simulation results of curved road with left turn.

6. CONCLUSION

In the field of electric drives with variable speed, an application of an electric vehicle controlled by an electronic differential is presented. This paper proposes an “independent machine" control structure applied to a propulsion system by a speed control. The results obtained by simulation show that this structure permits the realization of an electronic differential and ensures good dynamic and static performances. The electronic differential controls the driving wheels speeds with high accuracy either in flat roads or curved ones. The disturbances do not affect the performances of the driving motors.

Appendix

TABLE I: The Specification of Motor

Symbol	Parameter	Value
R	Resistance	0.03 Ω
L_d	d-axis inductance	2.10^{-4} H
L_q	q-axis inductance	2.10^{-4} H
Φ_f	Permanent magnet flux	0.08 Wb
p	Pole pairs	4

Abreviations

DTC : Direct Torque Control

EV : Electric Vehicle

MMS : Multi-machine Multi-converter System
MS : Mechanical Source
PMSM: Permanent Magnet Synchronous Machine

Nomenclature

L_d, L_q : d and q axis inductance

i_d, i_q : d and q axis currents

v_d, v_q : d and q axis voltage

R_s : Resistance

p : Pole pairs

θ : Electric position

Φ_f : Permanent magnet flux

J : Rotor inertia

J_v : Vehicle inertia

C_{em} : Electromagnetic torque

C_r : Load torque

M : Vehicle mass

R_r : Wheel radius

N_{red} : Report of speed gear

η : Transmission efficiency

l_w : Distance between two wheels and axes

d_w : Distance between the back and the front wheel

ρ : Air density

S : Front area of vehicle
C_x : Aerodynamic coefficient
g : Acceleration of gravity
f_r : Friction coefficient
α : Angle of the slope
v_h : Linear speed of vehicle
U_{dc} : Battery voltage

References

[1] A. Bouscaylor, B. Davat, B. de Fornel, B. Fraçois, "Multimachine Multiconverter System : application for electromechanical drives," *European Physic Journal – Applied Physics,* vol. 10, no. 2, May 2000, pp. 131-147.

[2] E., Benkhoris F., "Control structures for multi-machine multi-converter systems with upstream coupling, " *Elsevier, Mathematics and computers in simulation,* vol. 63, 2003, pp. 261-270.

[3] Y. Hori, senior member IEEE, "Future vehicles driver by electricity and control research on four wheel motored -UOT electric march II," *IEEE Transactions on Industrial Electronics,* vol. 51, no. 5, Oct. 2004, pp. 954 – 962.

[4] A. Bouscaylor, B. Davat, B. de Fornel, B. Fraçois, "Multimachine Multiconverter System for drives: analysis of coupling by a global modeling," *Proc. Of IEEE-IAS,* vol.3, 2000, pp.1474-1481.

[5] P. Pragasen, R. Krishnan. "Modeling, Simulation, and Analysis of Permanent Magnets Motor Drives, Part I: The Permanent Magnets Synchronous Motor Drive," *IEEE Transactions on Industry Applications*. .25 (2), 1989, 265-273.

[6] D.A.J. Rand, R. Woods, R.M. DELL. "Batteries for electric vehicles," *Research Studies*. Press Ltd. 1997.

[7] L.T. Lam, N.P. High, C.G. Phyland, A.J. Urban, Elservier, power sources, Vol. 144, pp. 552-555, 2005.

[8] L.T. Lam, R. Lovey, *Developpement of ultra-battery for hybrid-electric vehicle applications*, Elservier, power sources, Vol. 158, pp. 1140-1148, 2006.

[9] S. Kandler, C.Y. Wang, *Power and thermal characterization of Lithium-Ion battery pack for hybrid- electric vehicles*, Elservier, Power Sources, Vol. 160, pp. 662-673, 2006.

[10] T. Gillespice. "Fundamentals of vehicle dynamics," *Society of Automotive Engineers*, ISBN 1-56091-199-9.

[11] Cao, Xianqing, Zang, Chunhua, Fan, Liping, *Direct Torque Controlled Drive for Permanent Magnet Synchronous Motor Based on Neural Networks and Multi Fuzzy Controllers, IEEE International Conference on* Robotics and Biomimetics, 2006. ROBIO '06. Dec. 2006, pp. 197 – 201.

[12] T. Chapuis, D. Roy, S. Courtine. "Commande directe du couple d'une machine asynchrone par le contrôle direct de son flux statorique," *Journal de physique III* n°6, France, Juin 1995.

[13] M. Vasudevan, R. Arumugam, *New direct torque control scheme of induction motor for electric vehicles, 5th Asian* Control Conference, 2004. Vol. 2, 20-23 July 2004, pp. 1377 - 1383.